Journal of Applied Polymer Science

Influence of Curing Temperature on Properties of the Polyacrylonitrile/Polyimide Composite Films

Yaqin Chen, Baoping Lin, Hong Yang, Xueqin Zhang, Ying Sun
School of Chemistry and Chemical Engineering, Southeast University, Nanjing 211189, China
Correspondence to: B. Lin (E-mail: lbp@seu.edu.cn)

ABSTRACT: A series of polyacrylonitrile/polyimide (PAN/PI) composite films with different PAN contents are prepared under given curing temperatures (250, 300, 350, and 400°C). The microstructure of the composite films is observed by SEM, and the thermal, dielectric and mechanical properties of the composite films are determined. The results show that the self-assembly behavior of polyamic acid gives rise to connected network structure in the composite films and the variations in the microstructure of the composite films cured at different temperatures show important effects on the properties of PAN/PI composite films. © 2013 Wiley Periodicals, Inc. J. Appl. Polym. Sci. **2014**, *131*, 40283.

KEYWORDS: composites; films; polyimides; self-assembly

Received 16 October 2013; accepted 9 December 2013
DOI: 10.1002/app.40283

INTRODUCTION

Polyimide (PI) is a candidate polymer for a variety of applications such as packing materials, aerospace materials, circuit boards and interlayer dielectrics due to its good dielectric properties, flexibility, excellent thermal stability, high tensile strength, and good solvent resistance.[1–3] Composites incorporating the merits of each component have attracted tremendous interests.[4,5] In recent decades, polyimide nanocomposites, such as carbon nanotubes/PI composites,[6–9] graphene/PI composites[10–14] and inorganic oxide nanoparticle/PI composites,[15–18] have attracted much attention for their integration in mechanical property, thermal property, optical property, and electrical property of each component. But in the process of preparing these composites, the same problem occurs that the dopant can not be easily dispersed in the PI matrix for their compatibilities.

Polyacrylonitrile (PAN) is a semicrystalline organic polymer resin with a linear molecular structure. Though it is thermoplastic, PAN degrades before melting under normal condition. It can form highly oriented molecular structure when subjected to a low temperature heat treatment. Thermally induced reactions of PAN have been investigated by many researchers in the recent decades.[19–22] It has been widely accepted that the reactions can be divided into two stages: thermal stabilization and low temperature carbonization. Thermal stabilization usually occurs between 200 and 300°C and low temperature carbonization occurs between 300 and 900°C.[23] The heat treated PAN yields novel properties including, but not limited to, low density, enhanced electrical conductivity,[24] high tensile strength, and Young's modulus,[25–27] due to the cyclization and conjugation during heat treatment. It brings good applications in ultra filtration membranes,[28,29] hollow fibers for reverse osmosis[30,31] and fibers for textiles.[32] For its high tensile strength, PAN fibers are the most commonly adopted precursor for producing carbon fibers with superior tensile strength.[33–35] And researchers have also found that some functional groups, such as itaconic acid,[23] fluoro groups,[36] cobaltous chloride,[37] and methyl acrylate,[38] can lower the temperature for stabilization of PAN and increase its cyclization degree. The precursor of polyimide, polyamic acid (PAA) has carboxylic acid group which probably shows effect on the cyclization of PAN. And comparing to inorganic particles, PAN can easily disperse in the PI matrix. Doping PAN into the PI matrix is in hopes of incorporating the merits of the two and enhancing the dielectric property and mechanical property of the PI.

In this work, we prepared a series of PAN/PI composite films with different PAN contents under different curing temperatures. The thermo gravimetric analysis, dielectric constant, stress–strain curves and microstructure of the composite films were determined. According to the results of these determinations, we discuss the influence of curing temperature on the properties of the PAN/PI composite films.

EXPERIMENTAL

Materials

Pyromellitic dinahydride anhydride (PMDA, AR) and 4, 4′-diamino diphenyl ether (ODA, AR) were purchased from

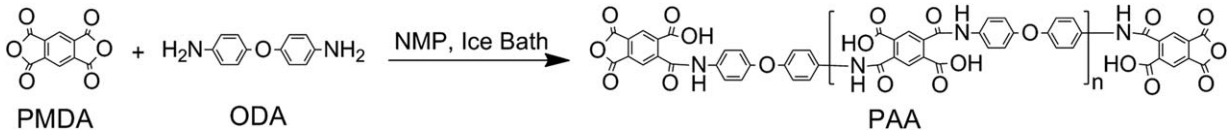

Scheme 1. Synthetic Route for PAA.

Sinopharm Chemical Reagent (Shanghai, China), and recrystallized from acetic anhydride and ethanol before use, respectively. PAN with average molecule weight of 150,000 was purchased from Aldrich. 1-methyl-2-pyrrolidone (NMP, AR) was obtained from Sinopharm Chemical Reagent (Shanghai, China) and was distilled over phosphorus pentoxide before use. CAN-24 conductive silver paste purchased from Cambridge Nanotech LTD (Xuzhou, China) was used as received.

Synthesis of Anhydride-Terminated Polyamic Acid (PAA)

ODA (19.046 g, 95.24 mmol) was added into a three-neck flask with distilled NMP (160 mL) under the protection of nitrogen. After the dissolution of ODA, the solution was cooled in an ice bath for 0.5 h. PMDA (20.962 g, 96.16 mmol) was added with vigorous stirring for 18 h. The synthetic route is shown in Scheme 1. The reaction mixture was diluted to 200 mL with NMP after maintained at room temperature for 36 h. The PAA solution (0.2 g/mL) was transferred in an amber bottom and reserved in a desicator for use.

Fabrication of the PAN/PI Composite Films

PAN was dissolved in NMP with given concentrations and then the PAN solution was added to a fixed quantity of PAA solution to yield a mixture with required PAN content. The contents of PAN in the composites were designed to 0, 2.5, 5.0, 7.5, and 10.0 wt %. The mixture was stirred with magnetic stirrer for 12 h at room temperature and followed by sonication in ultrasonic bath (100 W, 50%) for 0.5 h. Then the blend was cast into a glass mold. The glass mold was transferred to a vacuum oven and dried at 60°C for 5 h to remove NMP, and the PAN/PI composite film was cured at 150°C for 1 h and 250°C for 1 h stage by stage. The film prepared as described above was divided into four equal pieces. Three of them were respectively cured at 300, 350, and 400°C for 10 min in muffle furnace.

Measurements

The thermo gravimetric analysis (TGA) of the composite films was operated on TA Instruments SDT-Q600 with the heating rate of 10°C/min. And the tests were operated in N_2 atmosphere with the gas flow rate of 100 mL/min. Morphology of the cross-section of composite films was observed using FEI Sirion scanning electron microscope (SEM). Prior to observation, the specimens were wetting-off by liquid nitrogen and sprayed with gold nanoparticles by a BAL-TEC SCD005 sputter coater. Thicknesses of the composite films were measured by a digital thickness gauge (Time Group INC-TT230). Mechanical tests were conducted on a Rheometric Scientific DMTA5 at ambient temperature. And the composite films were cut into bone-shaped sheets. The upper grip was fixed and the lower grip descended at a rate of 0.6 mm/min. The dielectric constants of the composite films were tested with a Hioki 3532-50 impedance analysis instrument (Ueda, Nagano, Japan). Before this determination, the specimens of each kind of composites were cut into square with the length of 1 cm, and the thickness of each piece of samples was measured. Thereafter, conductive silver paste was brushed to a specific area on both sides of the specimen for dielectric constant testing. Following the same procedure described above, the specimen of pure PI was also prepared and tested for comparison.

RESULTS AND DISCUSSION

Thermal Properties of the Composite Films

To evaluate thermal properties of the composite films cured with different temperatures, thermo gravimetric analysis (TGA) of the composite films were determined. According the data of TGA, we calculated the derivative thermo gravimetry (DTG) curves and obtained the initial decomposition temperatures ($T_{initial}$), temperatures of maximum degradation (T_{max}) and residues at 800°C ($R_{800°C}$) of PI and PAN/PI composites. As shown in Figure 1(a), the pure PI films cured at 300, 350, and 400°C have no weight loss between 200 and 500°C, while the PI film cured at 250°C shows steady weight loss under that temperature range. This is because that the dehydration-cyclization happened during the imidization procedure of polyamic acid makes the weight of PI film loss, and the imidization of the polyamic acid can not completely finish until the curing temperature raised to 300°C or a higher temperature. Figure 1(b,e) show that the weight loss of the composite films cured at 250°C increases with the content of PAN between 200 and 500°C, while the TGA curves of 5.0 wt % PAN/PI composite films cured at 300, 350, and 400°C hardly show any weight loss in Figure 1(c). It means that the thermal stabilization of PAN is not totally finished at 250°C and the PAN/PI composite film cured at a temperature higher than 300°C shows thermo stability. The TGA curves of neat PI, 2.5, 5.0, 7.5, and 10.0 wt % PAN/PI composite films cured at 350°C are shown in Figure 1(d), and the relevant DTG curves of films cured at 350°C are shown in Figure 1(f). From the Figure 1(d,f), we can observe that the addition of PAN slightly decreases the thermo stability of PI.

Adding PAN into PI would slightly decrease the $T_{initial}$s of the composites, either the films are cured at 250 or 350°C, while the films cured at 350°C have much higher $T_{initial}$s than the films cured at 250°C (higher than 300°C), as shown in Table I. The $R_{800°C}$s of films cured at 350°C are also higher than those cured at 250°C. Although the addition of PAN slightly decreases the thermo stability of PI, the composite films still maintain good thermal stability ($T_{initial}$s > 500°C).

Microscopic Analysis

The morphology of the composites was investigated by SEM. Figures 2 and 3 present the cross-section images of neat PI and 5.0 wt % PAN/PI composite films with different magnifications. From the SEM images, it can be observed that the defects between the interfaces of the two polymers are not obvious

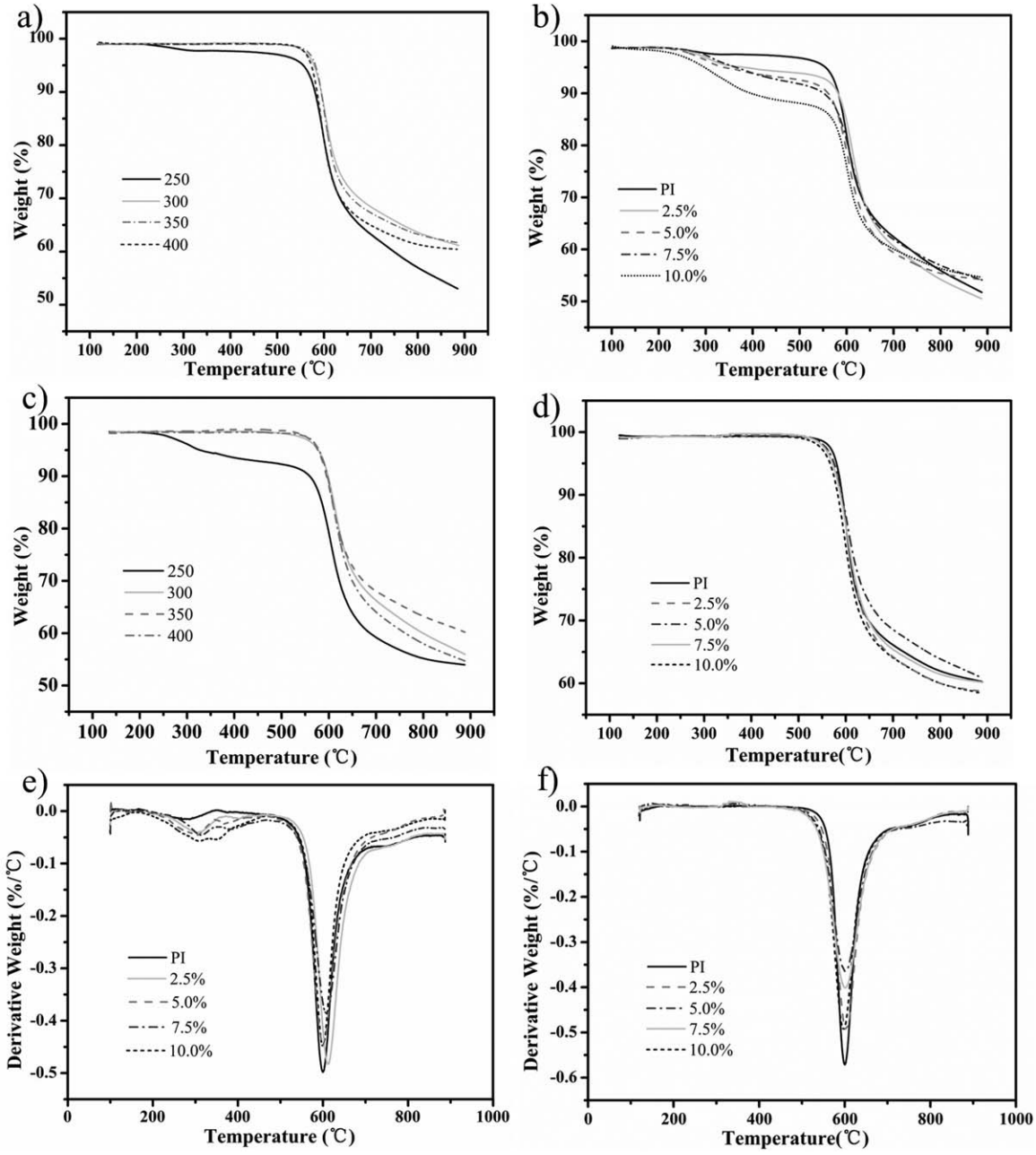

Figure 1. (a) TGA curves of neat PI cured at 250, 300, 350, and 400°C. (b) TGA curves of the composite films with different PAN contents cured at 250°C. (c) TGA curves of the 5.0 wt % composite films cured at 250, 300, 350, and 400°C. (d) TGA curves of the composite films with different PAN contents cured at 350°C. (e) DTG curves of the composite films with different contents cured at 250°C. (f) DTG curves of the composite films with different contents cured at 350°C.

when the films were cured at a lower temperature (250 and 300°C), and the PAN particles are well distributed throughout the films. The cross-sections of the PI films cured at both 250 and 400°C are very neat, as shown in Figure 2(a,d). The microstructures of the composite films cured at 250 and 300°C do not change obviously compared to the PI film. However, as the increase of the curing temperature (the composite film cured at either 350 or 400°C), an interesting phenomenon is observed that a connected network structure arises and runs throughout the cross-sections of the film as shown in Figure 2(e,f). These enormous differences can be interpreted from Figure 3 (the magnification of Figure 2).

When the PI film is cured at 250°C, a refreshing phenomenon is shown in Figure 3(a): lots of homogeneous rigid sphere particles are embedded in the cross-section of pure PI film. We hypothesize these rigid sphere particles are caused by self-assembly of PI. To the best of our knowledge, there are few reports about the self-assemble behavior of PI except X. Liu et al. find that polyimide bearing carboxy end-groups can

Table I. The Initial Decomposition Temperatures (*T*initial), Temperatures of Maximum Degradation (*T*max), and Residues at 800°C (*R*800°C) of PI and PAN/PI Composite Films Cured at 250 and 350°C

	$T_{initial}$ (°C)		T_{max} (°C)		$R_{800°C}$ (%)	
Sample	250°C	350°C	250°C	350°C	250°C	350°C
PI	199.5	541.7	599.9	599.9	56.72	62.05
2.5%	195.2	533.4	610.9	602.7	54.51	60.64
5.0%	194.5	530.3	600.4	602.7	55.97	64.91
7.5%	193.8	522.6	606.4	600.9	57.59	62.17
10.0%	185.5	517.8	599.7	597.5	56.49	60.33

self-assemble under low concentration in a single good solvent.[39] We believe the self-assemble mechanism of PI in this work is different from that reported by Liu et al, and this self-assembly may be caused by phase separation. We will continue to study this part of work in-depth in the future. When increasing the curing temperature of the PI film to 400°C, these rigid spheres disappear as shown in Figure 3(d). It could be caused for that the rigid spheres are destroyed after imidization and cross-linking reaction of polyamic acid as increasing the curing temperature.[40–42]

The addition of PAN obviously changes the microstructure of the PI. When the composite film is cured at 250°C, the interfaces between the spheres and the matrix become blurry. And when increasing its curing temperature to 300°C, the rigid spheres almost disappear and some rodlike particles arise in the composite film [square in Figure 3(c)] for the thermal stabilization of PAN molecule chain.[43,44] Figure 3(e,f) show the cross-sections of the composite films cured at 350 and 400°C, respectively. The rodlike particles in Figure 3(c) fade away while some quasi carbon whiskers appear in the matrix. The quasi carbon whiskers form connected network structure running throughout the films. These phenomena could be caused by the cyclization of PAN, which makes the PAN form conjugated structure. The conjugated macromolecule chain caused by the cyclization increases the differences of polarities between PAN and PI, which makes the molecule packing difficult, resulting in interfacial-phase separation.[20] Besides, some defects (lots of macropores) appear in the composite films as shown in Figure 3(e,f). Comparing to the composite film cured at 350°C, the macropores of the composite film cured at 400°C increase and the size of the macropore becomes larger. These defects are most likely caused for the free shrinkage behavior of PAN during the process of cyclization and cross-linking reaction.[45–48]

Dielectric Results

A complex dielectric permittivity consists of a real part and an imaginary part. The real part of the complex permittivity is often referred to as the dielectric constant (ε') and the imaginary part is referred to as the dielectric loss (ε''). The dielectric constant is a measure of the amount of energy from an external electrical field stored in the material, while the dielectric loss is a measure of the amount of energy dissipated in the dielectric material due to an external electric field. The total polarizability of the dielectric is the sum of the contributions due to several types of displacement of charges produced in the material by an applied field. Generally, the dielectric constant of a composite material arises as a result of the polarization of the molecules.

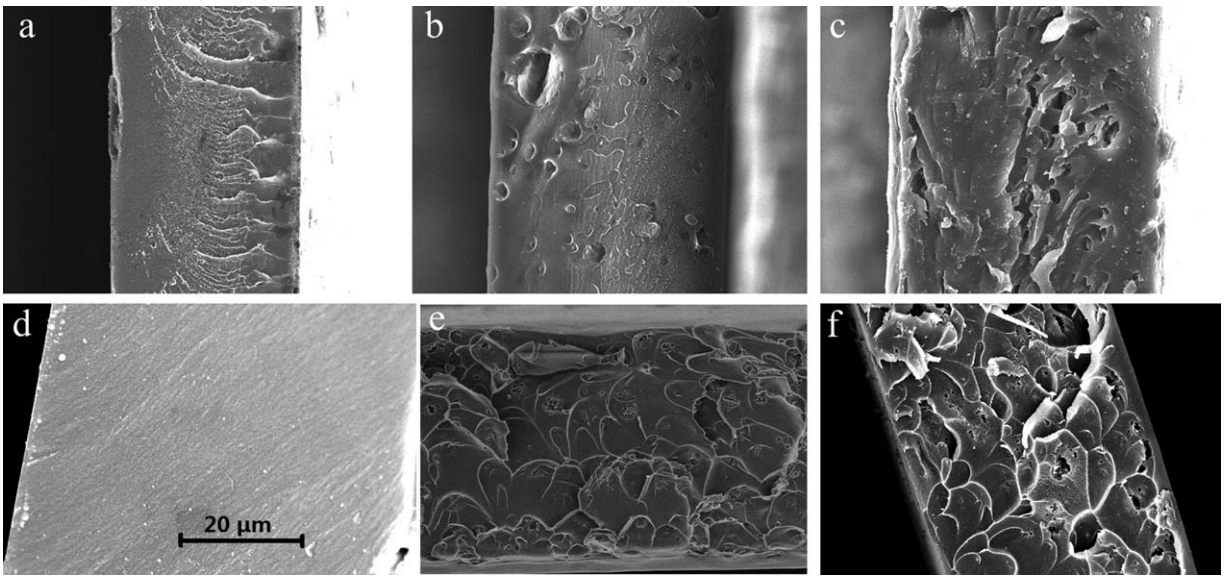

Figure 2. SEM of PI film cured at (a) 250°C, (d) 400°C, and 5.0 wt % PAN/PI composite films cured at (b) 250°C, (c) 300°C, (e) 350°C, (f) 400°C.

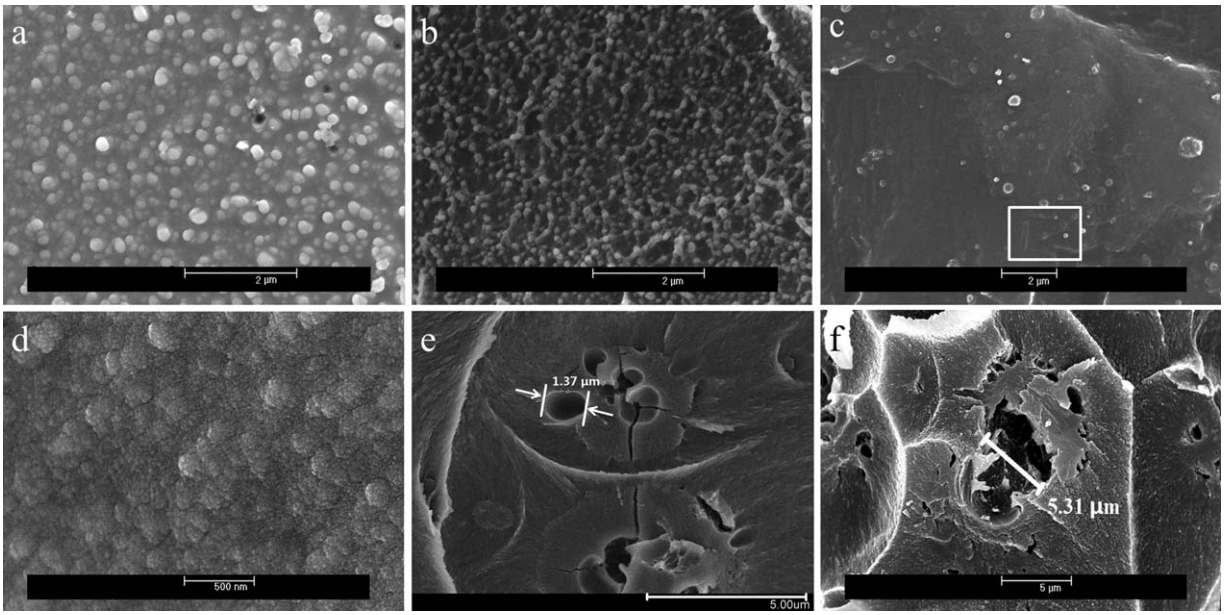

Figure 3. SEM with high magnification of PI film cured at (a) 250°C, (d) 400°C, and 5.0 wt % PAN/PI composite films cured at (b) 250°C, (c) 300°C, (e) 350°C, (f) 400°C.

The dielectric constant increases with an increase in the polarizability. The dielectric constant of a composite has contributions from interfacial, orientation, atomic, and electronic polarizations. The interfacial polarization occurs in a composite as a result of the difference in the conductivities or the polarizations of the matrix and fillers. The orientation polarization is produced when polymers containing polar groups are placed in an electric field. In this work, random oriented PAN doping in the PI matrix changes the structure of the total composite and leads to some physical effects in the composite such as the orientation and interfacial polarizations.[49]

To evaluate the dielectric property of the composite films, the devices were fabricated with the structure of silver paste/composite film/silver paste. And we only test dielectric properties of the films cured at 300, 350, and 400°C in this work, avoiding the error caused by self-assembly behavior of polyamic acid. Figure 4 shows the dielectric constants and dielectric losses of the composite films cured at different temperatures. When curing temperature of the films are 300 and 350°C, as shown in Figure 4(a,b), the dielectric constants increase with the addition of PAN in the PI matrix. It is mainly because that conjugated molecule chain of the cyclized PAN increases the differences of polarity between cyclized PAN and PI matrix, which enlarges the orientation and interfacial polarizations of the composite film. On the contrary, when curing temperature of the composite film reaches to 400°C, the dielectric constants decrease with the addition of PAN, as shown in Figure 4(c), for the increase of air macropores in the composite resulted by the shrinkage of PAN.[50–52] Usually the polarization decreases with the increase in frequency, this is the chief reason why the values of ε' increase with decreased frequency as shown in Figure 4.[53] The dielectric losses of the composite films were approximately 0.01. As described above, the cyclization of PAN will change the polarity of the PAN and make the PAN shrink, so optimizing curing temperature is particularly important for the preparation of the PAN/PI composite film.

Mechanical Properties

Typical stress–strain curves of the composite films cured at 350 and 400°C with different PAN contents are shown in Figure 5. When the PAN/PI composite films are cured at 350°C, the elongations of the films are enhanced first and then decrease as the PAN contents increase, while the tensile strengths of the composite films decrease first and then increase, as shown in Figure 5(a). The 2.5% PAN/PI composite film has the largest

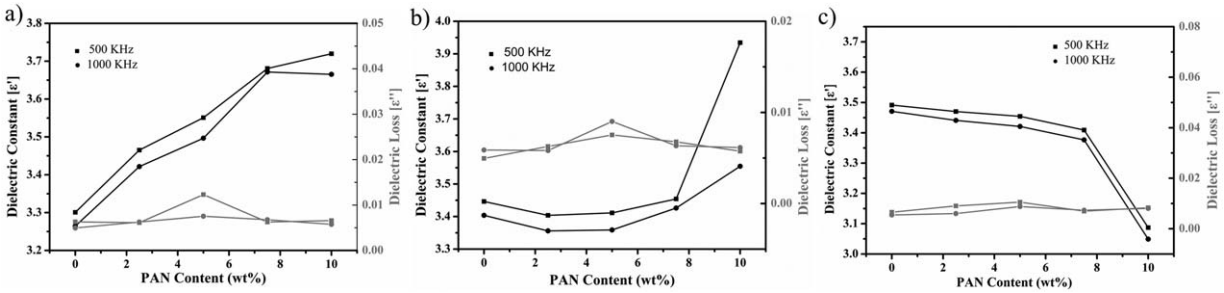

Figure 4. Dielectric constants and dielectric loss of the composite films cured at (a) 300°C, (b) 350°C and (c) 400°C.

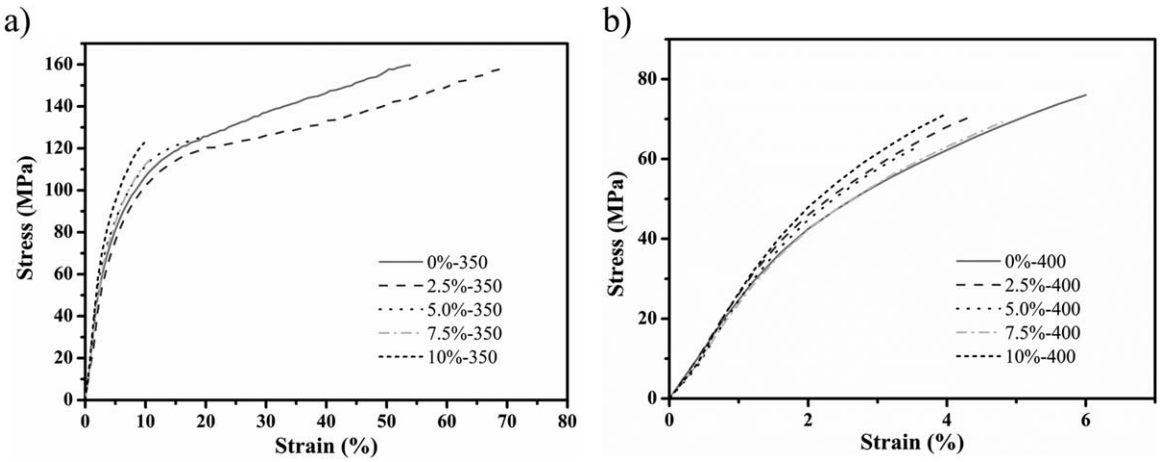

Figure 5. Tensile stress–strain curves of the PAN/PI composite films cured at (a) 350°C and (b) 400°C.

elongation and the lowest tensile strength. It is mainly because that the quasi carbon whiskers generated by the cyclization of PAN run through the PI matrix and they can form connected network structure easily as shown in Figure 2(e), which could enhance the mechanical property of the composite films.[20] Nevertheless, as the PAN content increases further, the defects of the composite films increase for the aggregation of cyclized PAN, and it will reduce the elongation of the composite films. When the curing temperature rises to 400°C, PAN shrinks obviously, while PI cannot deform with the PAN, which will leave lots of macropores in the composite films. This would reduce the mechanical properties of the films, even though the quasi carbon whiskers are helpful in enhancement of mechanical properties. As shown in Figure 5(b), the shrinkage behavior of PAN plays dominant role, and the elongations of the films are decreased sharply. The results show that the addition of PAN and the curing temperature can significantly change the mechanical properties of the PI film.

CONCLUSIONS

In conclusion, we prepared a series of PAN/PI composite films with different PAN contents and discussed the effect of curing temperature on properties of the composite film. When the films are cured at 250°C, an interesting phenomenon is found in the PI film: the incompletely imidized polyamic acid self-assembles to rigid sphere. This is conducive for PAN to distribute uniformly and form connected network structure throughout the PI matrix. As the curing temperature is raised to 350°C, the rigid spheres in the films disappear for imidization and cross-linking reaction, while 3D interconnected quasi carbon whiskers network arises in the composite films. The composite films cured at 350°C show enhanced mechanical property and increased dielectric constant. Further increasing the curing temperature to 400°C, many macropores are generated in the composite films for the shrinkage behavior of PAN, resulting that the dielectric constants and elongations of the composite films decreased. We hope this work will pave the way for an optimal solution to prepare PAN/PI composite materials.

ACKNOWLEDGMENTS

This research was supported in part by National Natural Science Foundation of China (Grant No. 21002012) and Jiangsu Provincial Natural Science Foundation of China (Grant No. BK2011588, BY2011153).

REFERENCES

1. Asano, N.; Aoki, M.; Suzuki, S.; Miyatake, K.; Uchida, H.; Watanabe, M. *J. Am. Chem. Soc.* **2006**, *128*, 1762.
2. Yuan, Y.; Lin, B. P.; Sun, Y. M. *J. Appl. Polym. Sci.* **2007**, *104*, 1265.
3. Lin, B. P.; Xu, X. H. *Polym. Bull. (Berlin)* **2007**, *59*, 243.
4. Xie, H. F.; Liu, B. H.; Yang, H.; Wang, Z. L.; Shen, J. Y.; Cheng, R. S. *J. Appl. Polym. Sci.* **2006**, *100*, 295.
5. Xu, X.; Xiao, H. N.; Guan, Y.; Li, S. Z.; Wei, D. F.; Zheng, A. N. *J. Appl. Polym. Sci.* **2013**, *127*, 959.
6. Song, C. W.; Jiang, D. W.; Li, L.; Sun, M. Y.; Wang, T. H. *J. Inorg. Mater.* **2012**, *27*, 923.
7. Wu, D. C.; Shen, L.; Low, J. E.; Wong, S. Y.; Li, X.; Tjiu, W. C.; Liu, Y.; Bin He, C. *Polymer* **2010**, *51*, 2155.
8. Im, H.; Yun, S.; Kim, *J. Polym. Compos.* **2011**, *32*, 368.
9. Chen, Y. Q.; Lin, B. P.; Yang, H.; Sun, Y.; Zhang, X. Q. *J. Polym. Sci., Part A: Polym. Chem.* **2013**, *51*, 3449.
10. Yoonessi, M.; Shi, Y.; Scheiman, D. A.; Lebron-Colon, M.; Tigelaar, D. M.; Weiss, R. A.; Meador, M. A. *ACS Nano* **2012**, *6*, 7644.
11. Liao, W. H.; Yang, S. Y.; Wang, J. Y.; Tien, H. W.; Hsiao, S. T.; Wang, Y. S.; Li, S. M.; Ma, C. C. M.; Wu, Y. F. *ACS Appl. Mater. Interfaces* **2013**, *5*, 869.
12. Shi, H. G.; Li, Y.; Guo, T. Y. *J. Appl. Polym. Sci.* **2013**, *128*, 3163.
13. Delvigs, P. *Polym. Compos.* **1989**, *10*, 134.
14. Hurwitz, F. I. *Polym. Compos.* **1983**, *4*, 90.
15. Yuan, Y. A.; Lin, B. P.; Sun, Y. M. *J. Appl. Polym. Sci.* **2011**, *120*, 1133.

16. Lin, B. P.; Liu, H. J.; Zhang, S. X.; Yuan, C. W. *J. Solid State Chem.* **2004**, *177*, 3849.
17. Lin, B. P.; Tang, J. N.; Liu, H. J.; Sun, Y. M.; Yuan, C. W. *J. Solid State Chem.* **2005**, *178*, 650.
18. Gao, L. X.; Li, L.; Qi, X. R.; Wei, W. X.; Hai, J. L.; Gao, W. Q.; Gao, Z. W. *Polym. Compos.* **2013**, *34*, 897.
19. Xue, Y.; Liu, J.; Liang, J. Y. *J. Appl. Polym. Sci.* **2013**, *127*, 237.
20. Kurmvanshi, S. K.; Gupta, A. K.; Patel, P. R.; Bajpai, R.; Keller, J. M. *Polym. Eng. Sci.* **2008**, *48*, 505.
21. Miao, P. K.; Wu, D. M.; Zeng, K.; Xu, G. L.; Zhao, C. E.; Yang, G. *Polym. Degrad. Stab.* **2010**, *95*, 1665.
22. Kim, J.; Kim, Y. C.; Ahn, W.; Kim, C. Y. *Polym. Eng. Sci.* **1993**, *33*, 1452.
23. Yu, M. J.; Wang, C. G.; Zhao, Y. Q.; Zhang, M.; Wang, W. Q. *J. Appl. Polym. Sci.* **2010**, *116*, 1207.
24. Al-Gurashi, M. A. M. *Pol. J. Chem.* **2001**, *75*, 689.
25. Zhang, W. X.; Liu, J.; Wu, G. *Carbon* **2003**, *41*, 2805.
26. Kostov, G. K.; Nikolov, A. T. *Polym. Compos.* **1994**, *15*, 367.
27. Qin, X. Y.; Lu, Y. G.; Xiao, H.; Zhao, W. Z. *Polym. Eng. Sci.* **2013**, *53*, 827.
28. Polotskaya, G. A.; Meleshko, T. K.; Novoselova, A. V.; Gofman, I. V.; Polotsky, A. E. *Pet. Chem.* **2012**, *52*, 527.
29. Li, G.; Xie, T. S.; Yang, S. L.; Jin, J. H.; Jiang, J. M. *J. Phys. Chem. C* **2012**, *116*, 9196.
30. Chung, T. S.; Kafchinski, E. R. *J. Appl. Polym. Sci.* **1996**, *59*, 77.
31. Mei, S. O.; Xiao, C. F.; Hu, X. Y. *J. Appl. Polym. Sci.* **2012**, *124*, E9.
32. Perepelkin, K. E. *Fibre Chem.* **2002**, *34*, 271.
33. Sedghi, A.; Farsani, R. E.; Shokuhfar, A. *J. Mater. Process. Tech.* **2008**, *198*, 60.
34. Shokuhfar, A.; Sedghi, A.; Farsani, R. E. *Mater. Sci. Technol.* **2006**, *22*, 1235.
35. Yu, M. J.; Xu, Y.; Wang, C. G.; Zhu, B.; Wang, Y. X.; Hu, X. Y.; Lin, X. *J. Appl. Polym. Sci.* **2012**, *124*, 5172.
36. Park, O. K.; Lee, S.; Joh, H. I.; Kim, J. K.; Kang, P. H.; Lee, J. H.; Ku, B. C. *Polymer* **2012**, *53*, 2168.
37. Ko, T. H.; Huang, L. C. *J. Mater. Sci.* **1992**, *27*, 2429.
38. Bang, Y. H.; Lee, S.; Cho, H. H. *J. Appl. Polym. Sci.* **1998**, *68*, 2205.
39. Liu, X. K.; Liu, J. Z.; Jiang, M. *Macromol. Rapid Commun.* **2009**, *30*, 892.
40. Liou, H. C.; Ho, P. S.; Tung, B. *J. Appl. Polym. Sci.* **1998**, *70*, 261.
41. Hsu, T. C. J.; Liu, Z. L. *J. Appl. Polym. Sci.* **1992**, *46*, 1821.
42. Jou, J. H.; Huang, P. T. *Macromolecules* **1991**, *24*, 3796.
43. Chatterjee, N.; Basu, S.; Palit, S. K.; Maiti, M. M. *J. Polym. Sci., Part B: Polym. Phys.* **1995**, *33*, 1705.
44. Fazlitdinova, A. G.; Tyumentsev, V. A.; Podkopayev, S. A.; Shveikin, G. P. *J. Mater. Sci.* **2010**, *45*, 3998.
45. Hou, Y. P.; Sun, T. Q.; Wang, H. J.; Wu, D. *J. Mater. Sci.* **2008**, *43*, 4910.
46. Gupta, A.; Harrison, I. R. *Carbon* **1996**, *34*, 1427.
47. Gupta, A.; Harrison, I. R. *Carbon* **1997**, *35*, 809.
48. Wang, B.; Zhao, C.; Xiao, S. J.; Zhang, J.; Xu, L. H. *J. Appl. Polym. Sci.* **2012**, *125*, 3545.
49. Rajesh, C.; Unnikrishnan, G.; Purushothaman, E.; Thomas, S. *J. Appl. Polym. Sci.* **2004**, *92*, 1023.
50. Aram, E.; Mehdipour-Ataei, S. *J. Appl. Polym. Sci.* **2013**, *128*, 4387.
51. Taki, K.; Hosokawa, K.; Takagi, S.; Mabuchi, H.; Ohshima, M. *Macromolecules* **2013**, *46*, 2275.
52. Karpagam, S.; Guhanathan, S.; Sakthivel, P. *Polym. Bull. (Berlin)* **2012**, *68*, 1023.
53. Yildiz, D. E.; Apaydin, D. H.; Toppare, L.; Cirpan, A. *J. Appl. Polym. Sci.* **2013**, *128*, 1659.